

Available online at [www.sciencedirect.com](http://www.sciencedirect.com)

**jmr&t**  
Journal of Materials Research and Technology  
[www.jmrt.com.br](http://www.jmrt.com.br)



## Original Article

# Manufacture of absorber fins for solar collector using incremental sheet forming

Rafael Gustavo Schreiber<sup>a,\*</sup>, Lirio Schaeffer<sup>b</sup>

<sup>a</sup> Instituto Federal de Santa Catarina (IFSC), Lages, Brazil

<sup>b</sup> Universidade Federal do Rio Grande do Sul (UFRGS), Porto Alegre, Brazil

### ARTICLE INFO

#### Article history:

Received 28 February 2018

Accepted 31 July 2018

Available online 19 October 2018

#### Keywords:

Incremental sheet forming (ISF)

Two point incremental forming (TPIF)

Solar collector

Parameter analysis

### ABSTRACT

This article sets out to present a new manufacturing process applied to create absorber fins for solar collectors. Using Incremental Sheet Forming, a flexible process that can be performed at a CNC production center, it is possible to make prototypes of absorber fins with collector riser fittings, which also enables the development of new fin designs using different materials in a wide range of thicknesses. This article analyzes parameters of the Two Point Incremental Forming process, with a partial die for solar collector absorber fin manufacturing using a 1 mm thick aluminum AA1200-H14 in order to determine the influence of the step down and the tool's rotation speed on the sheet's formability, being thus able to determine the most appropriate combination of these parameters to obtain a process with the greatest quality and productivity. A series of 16 experiments was proposed to manufacture a small absorber fin comparing the rotation speed values of  $S = 50, 200, 400,$  and  $800$  rpm, with step down values of  $\Delta z = 2, 1, 0.5,$  and  $0.2$  mm. The feed rate value was kept at  $F = 250$  mm/min, and each experiment was performed until the first crack occurred in the sheet. In this study, it was possible to indicate the feasibility of the process under more efficient parameters for manufacturing absorber fins using the step down of 2 mm and the rotation speed of 50 rpm.

© 2018 Brazilian Metallurgical, Materials and Mining Association. Published by Elsevier Editora Ltda. This is an open access article under the CC BY-NC-ND license (<http://creativecommons.org/licenses/by-nc-nd/4.0/>).

## 1. Introduction

Incremental sheet forming is a process applied to quick prototyping or to the manufacturing of pieces in small lots [1–3] as it presents greater flexibility and greater formability compared to the conventional forming process [3]. This process

has been used in different applications such as panel manufacture for special cars [4], cranial implants prototypes [5], and development of new models of solar collectors [6]. This article presents a case study using the incremental sheet forming process applied to absorber fin manufacturing for flat plate solar collectors. It has been selected because it allows rapid

\* Corresponding author.

E-mails: [rafael.schreiber@ufrgs.br](mailto:rafael.schreiber@ufrgs.br) (R.G. Schreiber), [schaefer@ufrgs.br](mailto:schaefer@ufrgs.br) (L. Schaeffer).

<https://doi.org/10.1016/j.jmrt.2018.07.018>

2238-7854/© 2018 Brazilian Metallurgical, Materials and Mining Association. Published by Elsevier Editora Ltda. This is an open access article under the CC BY-NC-ND license (<http://creativecommons.org/licenses/by-nc-nd/4.0/>).

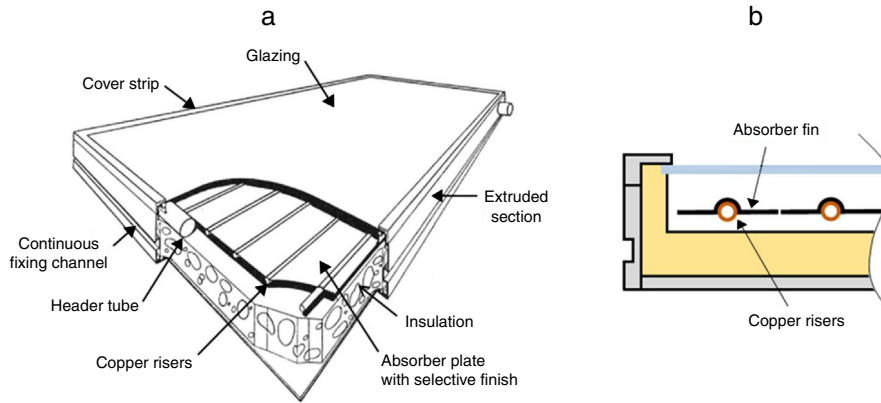


Fig. 1 – Typical water-heating flat plate collector panel (a) [8], and assembly detail of absorber fin on the copper risers (b).

prototyping and eliminates the use of complex and expensive tools.

The flat plate collector in residential applications is generally used for heating bath water in temperature ranges between 30 °C and 80 °C [7]. These collectors are formed by a serpentine, which is constituted by various copper risers welded to two other risers with a larger diameter, through which the fluid to be heated flows. The serpentine is mounted in a box formed by extruded sections on the sides and a plate at the bottom, both overlaid with thermal isolation in order to diminish the system’s thermal losses. A glass cover in the upper part of collector allows solar radiation to pass through in order to heat the fluid, reducing the convective and radiative losses.

The risers can be covered by a single absorber plate welded to them or by several fitted absorber fins. Fig. 1a shows a model of a closed flat plate collector and its components while Fig. 1b shows a detail of the assembly of absorber fins on the copper risers.

The absorber fins mounted on the copper risers are used to absorb solar radiation, which is transmitted by the glass and is conducted to the copper risers. For this reason, they are painted with matte black paint or coated to form a selective surface.

For absorber fins with fittings for the risers’ serial production the rolling process could be applied. However, with

incremental sheet forming it is possible to perform quick prototyping of absorber fins, enabling the development of new designs in a wide range of thicknesses due to process flexibility.

Incremental sheet forming consists on the progressive forming of a flat sheet metal with  $s_0$  thickness and of a  $\Delta z$  step-down with a  $d_t$  diameter semispherical tip forming tool. In this process, the plate is fixed between the blank-holder and backing plate (positioned over a rig). The opening of the backing plate determines the forming tool’s work surface without the mandatory use of the die in the lower part of the device. As the forming tool rotates, it penetrates the sheet vertically, as shown in Fig. 2.

In order to obtain the formed piece final configuration several tool increments are needed, and their path can be carried out at a CNC production center [2,3]. By incrementing the tool over the sheet, a wall angle  $\psi$  is formed with the horizontal axis and a wall angle  $\lambda$  is formed with the vertical axis. The wider the angle  $\psi$ , the smaller will be angle  $\lambda$ , and the smaller will be the final thickness ( $s_1$ ) of the formed sheet.

Various parameters used in the process have great influence on the quality of the formed product, such as tool diameter, sheet thickness, lubrication, process temperature, wall angles [10,11], step down, rotation speed (S) and feed rate (F). In this study, some of these parameters were analyzed in order to obtain greater productivity and qual-

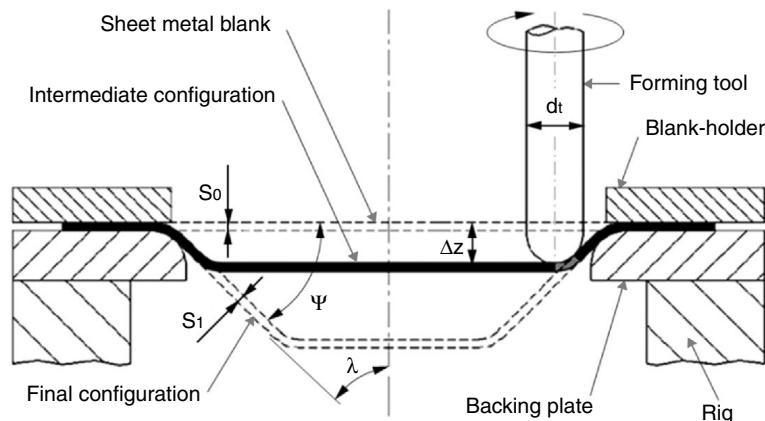


Fig. 2 – Incremental sheet forming schematic representation [9].

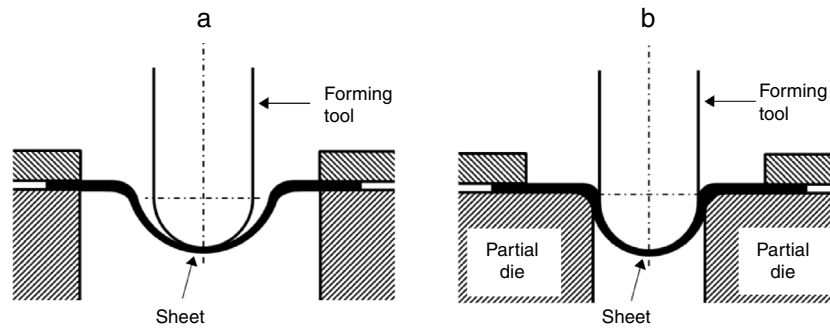


Fig. 3 – Sheet conformed by SPIF (a) and by TPIF (b).

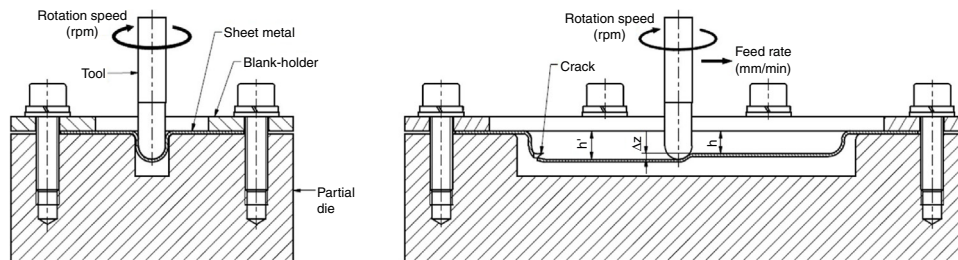


Fig. 4 – Experiment for analysis of the incremental sheet forming parameters.

ity in manufacturing absorber fins using incremental sheet forming.

According to studies by Bhattacharya et al., the larger the tool diameter, the smaller the roughness of the formed sheet [12]. In the study by Al-Ghamdi and Hussain, a critical radius  $R_c$  was determined for an incremental sheet forming tool. In this study it was found that the value of the tool radius influences the formability of the sheet in the incremental sheet forming process, and that its value does not depend on the type of material or on the sheet's mechanical properties, but rather on blank thickness, so that the critical radius for forming with a maximum wall angle with better formability is obtained based on the initial blank thickness by the  $R_c \approx 2.2 \cdot s_0$  relation. As the tool radius value moves away from this relation, sheet rupture becomes more imminent [13].

In the study by Azevedo et al., various lubricants for incremental sheet forming were compared, and it was concluded that in incremental sheet forming of aluminum SAE 30 mineral oil and AL-M grease [14] obtained lower roughness and force values.

Studies performed on the application of heat on the material to be formed concluded that it is possible to significantly reduce the efforts in forming [15] and springback at certain forming temperatures [16,17].

In the study by Garg et al. [1], it was found that sheet thickness and wall angle are the parameters with the greatest influence on strain energy and geometric precision.

## 2. Experimental procedure

In order to perform a broad analysis of the rotation speed influence and the step down parameters on the incremental sheet

forming process for absorber fin manufacturing, a series of 16 experiments with a Two-Point Incremental Forming (TPIF) partial die were proposed to manufacture a small absorber fin, comparing different parameter combinations. The objective of using TPIF with the partial die was to ensure the formed absorber fin's precision by restricting its geometry to the form proposed in order for it to fit the collector riser, which would not be possible using Single Point Incremental Forming (SPIF) since it presents smaller dimensional accuracy, according to Fig. 3.

In these experiments, the rotation speed values of  $S = 50, 200, 400,$  and  $800$  rpm, and the step down values of  $\Delta z = 2, 1, 0.5,$  and  $0.2$  mm, were selected, bringing it to a total of 16 experiments. A feed rate of  $F = 250$  mm/min was used in all experiments, due to the fact that this parameter had little influence on formability and roughness [18,19].

Each experiment was performed until the first crack occurred in the material, considering the depth value at the time the crack occurred as  $h'$  and the depth of the forming tool without cracks as  $h$ . The material selected for the experiment was a sheet of AA1200-H14 aluminum with the following dimensions:  $1 \times 60 \times 160$  mm. This was fixed between a partial die and a blank-holder, as indicated in Fig. 4.

The machine selected for the experiments was a ROMI CNC production center, Discovery 4022 model, with longitudinal travel - X axis of 559 mm, cross travel - Y axis of 406 mm and vertical travel - Z axis of 508 mm.

The forming tool was manufactured from High Speed Steel with a semispherical 9.525 mm tip diameter (the same dimension as the diameter of the absorber fin fitting riser), in order to minimize fin roughness and forming time.

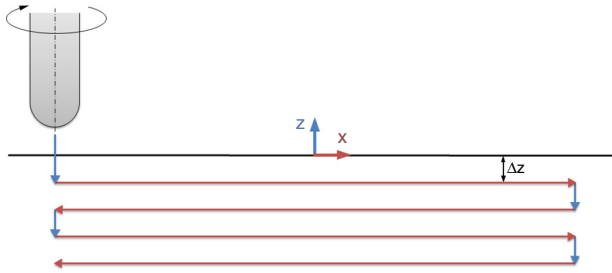


Fig. 5 – Tool path in the experiments.

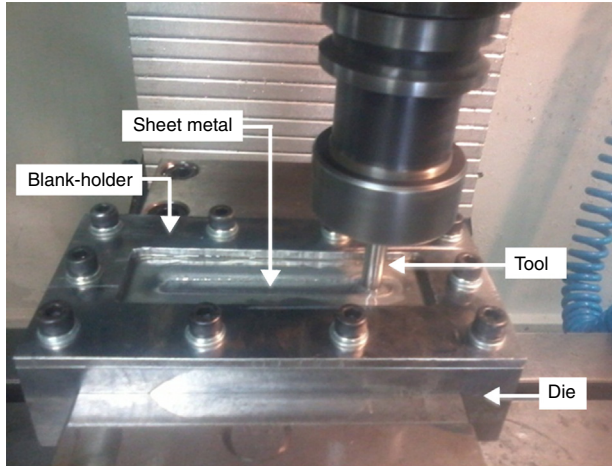


Fig. 6 – Incremental sheet forming process being performed at the CNC production center.

A simple path was defined for the forming tool using CAM software programming, through which movements were performed on the Z and X axes as indicated in Fig. 5. In this way, after each step down the tool was displaced longitudinally until a new step down was performed on the opposite side. The experiment was interrupted when the sheet presented a crack.

The ISO VG 100 oil, equivalent to the SAE 30 oil, was used for lubrication in this process. It presented good results in the experiments by Azevedo et al. [14].

The output parameters analyzed, besides the depths  $h$  and  $h'$ , were the final thickness of the sheet, the strains  $\varphi_1$  and  $\varphi_2$ , and the temperature during the process (measurement with an optical pyrometer).

All tested specimens were electrochemically engraved with  $\varnothing 2.5$  mm circles in order to analyze strains after forming. Fig. 6 presents the incremental sheet forming process that was performed in the CNC Production Center.

The pure aluminum AA1200-H14 was selected for this study due to its high thermal conductivity, essential property for the application in solar collectors. Table 1 presents uniaxial tensile mechanical properties, thermal conductivity and hardness of the as-received material as well as the blank sheet's initial average roughness.

### 3. Results and discussion

#### 3.1. Incremental sheet forming parameters

Based on the 16 experiments performed, the input parameters (step-down  $\Delta z$  and rotation speed  $S$ ) were compared to the output parameters (depth without crack  $h$ , depth up to the crack  $h'$ , final thickness of the sheet  $s_1$ , major strain  $\varphi_1$ , minor strain  $\varphi_2$ , temperature variation  $\Delta T$ , and if any material was removed in the form of powder in the process), as indicated in Table 2.

At the moment of the crack, verified by visual inspection, the CNC machine panel recorded the depth ( $h'$ ), and by subtracting the step down value ( $\Delta z$ ), the depth value without crack ( $h$ ) was determined according to Eq. (1).

$$h = h' - \Delta z \tag{1}$$

In the first four experiments (with a step down of  $\Delta z = 2$  mm and rotation speed varying from  $S = 50$  to 800 rpm) the formed region remained without cracks until the depth of  $h = 6$  mm was reached, while in the next increment of  $h' = 8$  mm, the crack appeared catastrophically, accompanying the displacement of the tool towards the site where the experiment was interrupted. In these experiments, the strains obtained indicated high values of plane-strain with  $\varphi_1 = 0.69$  and  $\varphi_2 = 0$ , measured next to each crack. Although these strains have the same values in all four experiments, it can be observed that as the rotation speed increased the crack openings diminished, as shown in Fig. 7.

In the other experiments with smaller step downs, greater strains occurred up to the beginning of cracks (with  $\varphi_1$  values from 0.79 to 0.96) maintaining the strain  $\varphi_2 = 0$ . In experiments 5–16 the cracks are seen only at the site of vertical tool penetration. It can also be observed that as the rotation speed increased, combined with step down reduction, greater strains were obtained and the cracks observed were also smaller, as shown in Fig. 8.

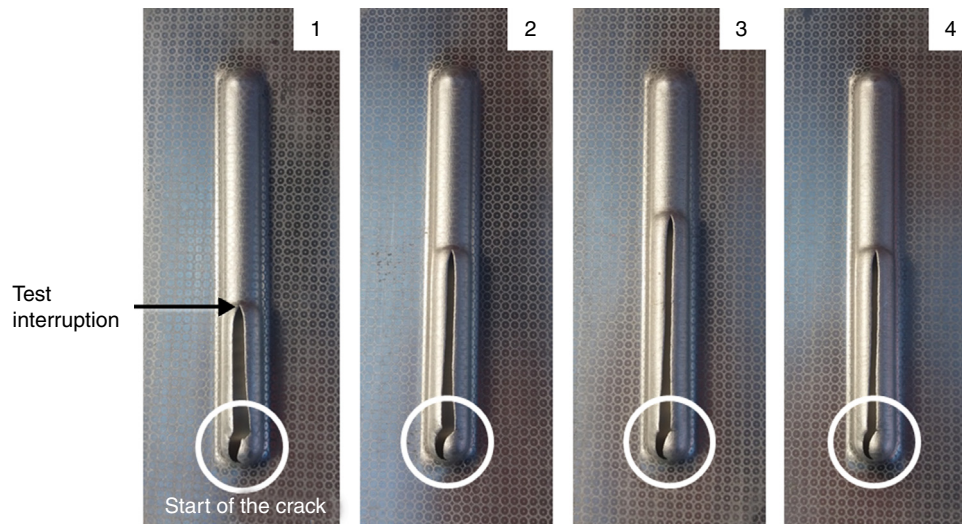
Based on these results, it is possible to establish a relation between depth without a crack ( $h$ ) and rotation speed ( $S$ ) in each experiment, as indicated in Fig. 9. It thus becomes clear that in large step downs there is little influence of rotation speed at the depth without cracks, while in small increments this influence becomes significant. Generally, the greater the

Table 1 – Properties of the AA1200-H14.

Yield strength (MPa)	Tensile strength (MPa)	Elongation (%)	Modulus of elasticity (GPa)	Strain-hardening exponent	Hardness (HB)	Roughness Ra ( $\mu\text{m}$ )	Thermal conductivity (W/m.K)
95	110–145	1–3	70	0.047	35	0.50	222

**Table 2 – Analysis of parameters in incremental sheet forming AA1200-H14.**

N°	$\Delta z$ (mm)	S (rpm)	h (mm)	h' (mm)	s <sub>1</sub> (mm)	$\varphi_1$	$\varphi_2$	$\Delta T$ (°C)	Metal powder?
1	2	50	6	8	0.50	0.69	0	0	No
2	2	200	6	8	0.50	0.69	0	1.1	No
3	2	400	6	8	0.50	0.69	0	2.3	No
4	2	800	6	8	0.50	0.69	0	3.6	Yes
5	1	50	6	7	0.45	0.79	0	0.1	No
6	1	200	6	7	0.45	0.79	0	0.2	No
7	1	400	6	7	0.45	0.79	0	3.2	No
8	1	800	6	7	0.45	0.79	0	2.5	Yes
9	0.5	50	6.5	7	0.41	0.88	0	0	No
10	0.5	200	6.5	7	0.41	0.88	0	0.7	No
11	0.5	400	6.5	7	0.41	0.88	0	2.2	Yes
12	0.5	800	7	7.5	0.40	0.92	0	5.3	Yes
13	0.2	50	6.6	6.8	0.44	0.83	0	0	No
14	0.2	200	6.8	7	0.41	0.88	0	1.2	Yes
15	0.2	400	7	7.2	0.40	0.92	0	3.1	Yes
16	0.2	800	7.6	7.8	0.38	0.96	0	4.3	Yes

**Fig. 7 – Beginning of cracks in experiments 1– 4.**

rotation speed, the greater will be the depth formed without a crack. However, considering that there is little variation in the results for this type of material, depending on the depth of the canal to be formed, it may be more productive to use greater step downs to obtain shorter periods of time to manufacture the piece.

The study reached the conclusion that the temperature variation in the contact region between the sheet and the forming tool was practically nil in the experiments performed with rotation speed of  $S = 50$  rpm, and that it increased little as the rotation gained speed and the increment diminished, reaching a maximum variation of  $\Delta T = 4.3^\circ\text{C}$  in the 16th experiment, and  $\Delta T = 5.3^\circ\text{C}$  in the 12th experiment. Considering the ambient temperature of  $20^\circ\text{C}$  in the laboratory where the experiments were performed, it was concluded that the maximum temperature obtained was much lower than the recrystallization temperature of the material and, therefore, temperature variation was insignificant to influence the material formability. As such, in the analyzed parameter range, the increased formability may be more closely related to the variation of friction (that which occurs with the rotation speed

variation) than with the increase in temperature. This finding is related to the study by Xu et al. [20], in which, in the AA5052-H32 forming, it was found that friction plays an essential role in increasing formability at rotation speeds between 0 and 1000 rpm, while between 2000 and 7000 rpm temperature variation becomes predominant. Consequently, in this study, it was also concluded that, in general, the depth at which the fracture occurs is greater as the tool rotation speed increases.

Fig. 10 indicates the relation between the depth without a crack ( $h$ ) and the step down ( $\Delta z$ ) in each experiment, where it can be observed that, in all cases, the greater the increment, the smaller the formed depth without a crack. It can also be observed that the rotation speed only presents a significant influence combined with small step down values.

The reduction in sheet formability (measured by the formed piece angle) as a direct consequence of the increased step down is also indicated in the study by Bhattacharya et al. [12].

The Forming Limit Curve (FLC) was determined by the Nakajima test, in which eight specimens with dimensional

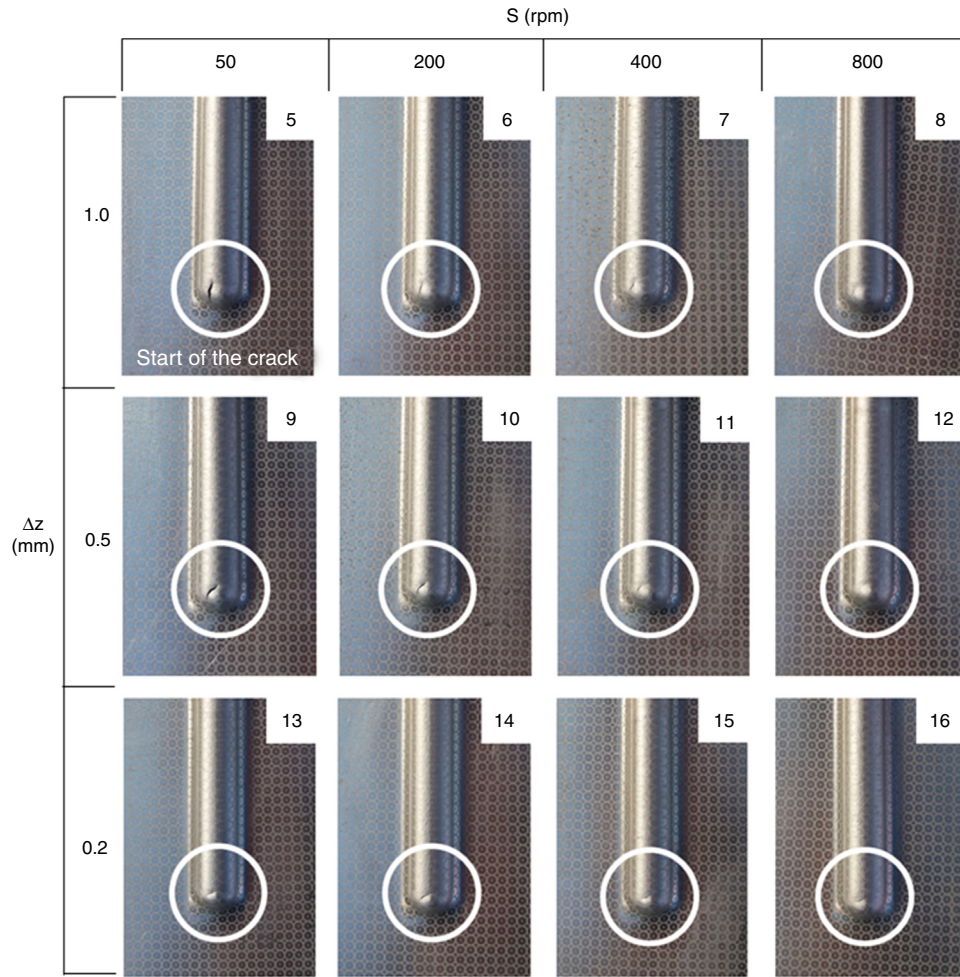


Fig. 8 – Beginning of cracks in experiments 5-16.

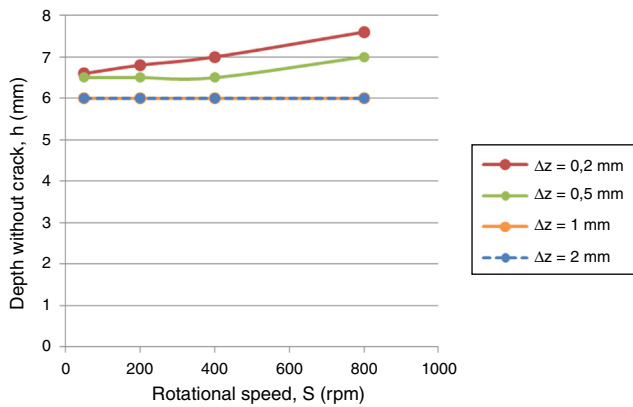


Fig. 9 – Relation between depth without a crack (h) and rotation speed (S) in the incremental sheet forming experiments.

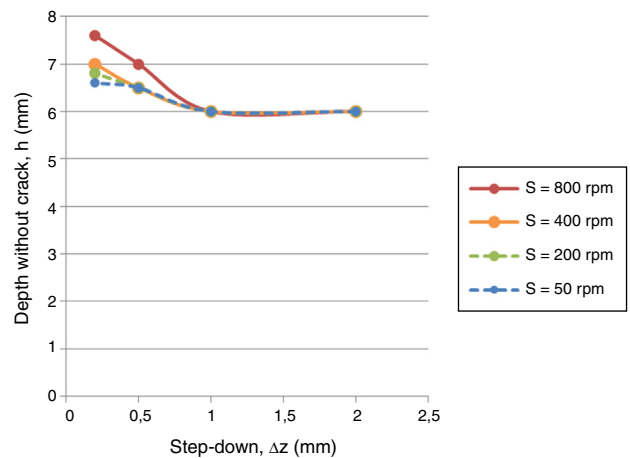


Fig. 10 – Relation of depth without a crack (h) and step down (Δz) in the incremental sheet forming experiments.

variation of width and radius were stamped, and all the specimens were electrochemically engraved. The deformations  $\varphi_1$  and  $\varphi_2$  were measured after the test forming the FLC added in Fig. 11. The strains obtained in incremental sheet forming with all parameters combinations were much greater than those

obtained by the FLC, which confirms the studies by Kim and Park [3]. The major strain ( $\varphi_1 = 0.96$ ) was obtained in the 16th experiment with values of  $\Delta z = 0.2$  mm and  $S = 800$  rpm. In this configuration, the depth formed without a crack was 7.6 mm.

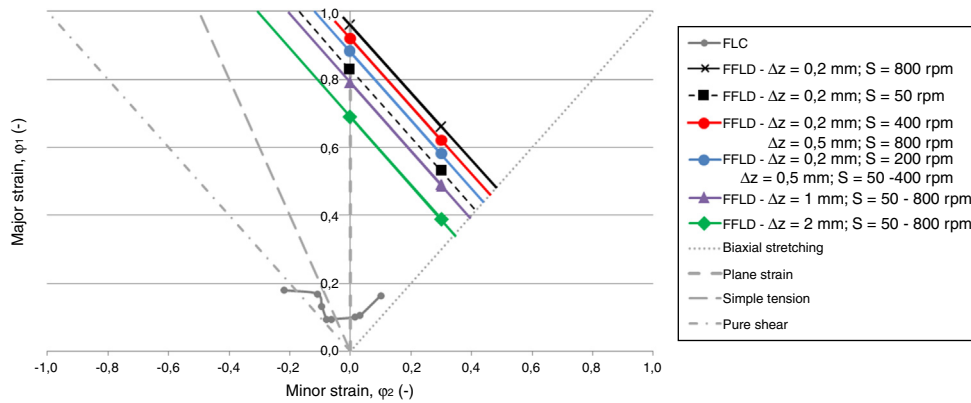


Fig. 11 – Comparison of strains obtained in FLC and FFLD for AA1200-H14.

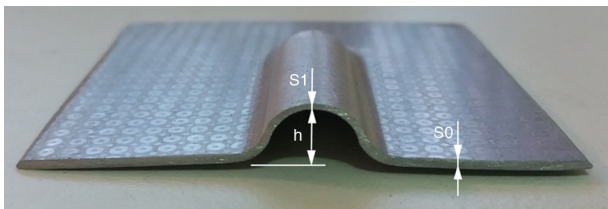


Fig. 12 – Variation of thickness in the formed sheet.

Fig. 11 also shows the Fracture Forming Limit Diagram (FFLD) obtained in each experiment. In some cases more than one experiment had the same deformation, so they were grouped in the same FFLD, such as the 12th experiment (with  $\Delta z = 0.5$  mm and  $S = 800$  rpm), which presented the same strain as the 15th experiment (with  $\Delta z = 0.2$  mm and  $S = 400$  rpm). Experiments 9 to 11 (with  $\Delta z = 0.5$  mm and  $S = 50$  to 400 rpm) also presented the same strain as the 14th experiment (with  $\Delta z = 0.2$  mm and  $S = 200$  rpm). Thus, it can be verified that it was more productive to use  $\Delta z = 0.5$  mm than  $\Delta z = 0.2$  mm, which enabled forming in a shorter period of time with the same strains and basically the same depth formed until the cracks appeared. On the other hand, the smaller strains were obtained with  $\Delta z = 2$  mm and  $\Delta z = 1$  mm, regardless of the rotation speed used.

It was also found that as the step down diminished and rotation speed increased, material was removed in the process, which may indicate that the lubricant was not efficient under these conditions. The material removed in the form of powder was mixed with the lubricant oil, which made it difficult to make visual confirmation of even the moment when the crack occurred in the experiment.

As expected, the initial thickness  $s_0$  of the sheet formed by the incremental process is reduced to thickness  $s_1$ . This parameter is shown in the sheet section as indicated in Fig. 12, where  $h$  was considered the depth at which no crack occurred.

The final formed piece satisfactorily complied with the aimed design, without significant deviations that could compromise the fit of the fin with the copper riser. The decrease in thickness was constant, with the lowest value at the top of the fin, as shown in Fig. 12. In this region, it was difficult to measure the thickness with the pachymeter, since it

required cutting all sheets. It was then decided to obtain the final thickness value by calculation.

To obtain final thickness  $s_1$  values it was necessary to first define the deformation in the thickness  $\varphi_3$ . This is calculated by considering the constant volume law, which defines that the sum of the deformations is equal to zero, according to Eq. (2).

$$\varphi_1 + \varphi_2 + \varphi_3 = 0 \quad (2)$$

Since the deformations  $\varphi_1$  and  $\varphi_2$  were obtained experimentally, one can isolate  $\varphi_3$ , determining its value, according to Eq. (3).

$$\varphi_3 = -(\varphi_1 + \varphi_2) \quad (3)$$

Considering that the deformation  $\varphi_3$  is obtained by the natural logarithm of the product between the final thickness and the initial thickness, according to Eq. (4).

$$\varphi_3 = \ln \frac{s_1}{s_0} \quad (4)$$

We can then isolate the final thickness ( $s_1$ ) by Eq. (5) and Eq. (6).

$$\frac{s_1}{s_0} = e^{\varphi_3} \quad (5)$$

$$s_1 = e^{\varphi_3} \cdot s_0 \quad (6)$$

Eq. (6) was used to calculate the final thicknesses with values between 0.38 mm and 0.50 mm, as indicated previously in Table 2. Although very small, this variation presented a relation to the formed depth, as indicated by Martins et al. [9], and the higher the value of the formed depth, the lower the value of the final thickness.

### 3.2. Manufacturing the prototype

Among the parameters analyzed in this study, the step down value of  $\Delta z = 2$  mm was chosen since it enabled forming in a shorter period of time and it was able to reach the necessary depth to fit the absorber fin in the riser. The rotation selected

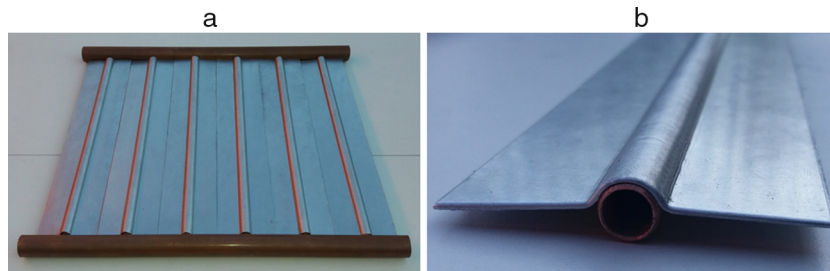


**Fig. 13 – Prototype of the serpentine with absorber fins (a) and detail of formed absorber fin over the riser fitting (b).**

was  $S = 50$  rpm, due to the fact that the rotation speed does not significantly influence the formability when a greater step down is used. Moreover, greater rotation speed could generate excessive friction and consequently the removal of material, as indicated in Table 2.

In order to analyze the application of the absorber fin manufactured by incremental sheet forming, a serpentine prototype was built with copper risers and absorber fins were fitted over it. The absorber fins were manufactured with  $1 \times 60 \times 300$  mm sheets, as indicated in Fig. 13a. Fig. 13b shows the detail of the absorber fin mounted on the copper riser, where it can be seen that the fitting was performed satisfactorily, meeting the proposal of the study.

The incremental sheet forming was done up to the depth of 5 mm without any cracks occurring in the sheet, as had already been foreseen by the previous analysis.

#### 4. Conclusions

This work presented a new alternative for a manufacturing process applied to solar collectors' absorber fins. Through a broad analysis of the incremental sheet forming process parameters in this application, the following conclusions were reached:

1. Compared to conventional forming, incremental sheet forming presents greater formability;
2. Combining high rotation with a small step down, it is possible to obtain greater strains until cracks appear in the sheet;
3. The greater the rotation and the smaller the step down, the greater the chances that some of the material will be removed in the form of powder in the process, which may indicate inefficient lubrication;
4. It is possible to determine the formed sheet final thickness through relation of constant volume, which is very important for the development of new products from a practical point of view;
5. Although greater strains can be obtained with greater rotation speeds and smaller step downs, in the case of the prototype manufactured for this study it was possible to obtain the desired geometry with a high increment, which made the process much more productive. However, the prototype with the best quality was achieved with less rotation speed, in which case there was no removal of material in the form of metallic powder. As such, the

most appropriate parameter combination in this case was with a step down of  $\Delta z = 2$  mm and a rotation speed of  $S = 50$  rpm.

#### Conflicts of interest

The authors declare no conflicts of interest.

#### Acknowledgments

The authors would like to thank Prof. Dr. Elizabeth Marques Duarte Pereira at the UNA University Center in Belo Horizonte for her support in revising this work and for her contributions in the field of solar heating systems in Brazil.

#### REFERENCES

- [1] Garg A, Gao L, Panda BN, Mishra S. A comprehensive study in quantification of response characteristics of incremental sheet forming process. *Int J Adv Manuf Technol* 2016;89:1353–65.
- [2] Li Y, Chen X, Liu Z, Sun J, Li F, Li J, et al. A review on the recent development of incremental sheet-forming process. *Int J Adv Manuf Technol* 2017;92:2439–62.
- [3] Park JJ, Kim YH. Fundamental studies on the incremental sheet metal forming technique. *J Mater Process Technol* 2003;140:447–53.
- [4] Amino M, Mizoguchi M, Terauchi Y, Maki T. Current status of “Dieless” Amino’s incremental forming. *Procedia Eng* 2014;81:54–62.
- [5] Castelan J, Schaeffer L, Daleffe A, Fritzen D, Salvato V, Da Silva FP. Manufacture of custom-made cranial implants from DICOM® images using 3D printing CAD/CAM technology and incremental sheet forming. *Revista Brasileira de Engenharia Biomedica* 2014;30:265–73.
- [6] Arruda RP, Baroni A, Shaeffer L. Sheet metal forming: new technologies applied to the fabrication of solar energy collector panels. *Int J Mechatron Manuf Syst* 2008; 1:254–63.
- [7] Kalogirou SA. *Solar energy engineering: processes and systems*. 2nd ed. San Diego: Academic Press; 2014.
- [8] Norton B. *Solar Energy Thermal Technology*. New York: Springer-Verlag; 1992.
- [9] Martins PAF, Bay N, Skjoedt M, Silva MB. Theory of single point incremental forming. *CIRP Ann Manuf Technol* 2008;57:247–52.
- [10] Jiménez I, López C, Martínez-Romero O, Mares P, Siller HR, Diabb J, et al. Investigation of residual stress distribution in single point incremental forming of aluminum parts by X-ray diffraction technique. *Int J Adv Manuf Technol* 2017;91:2571–80.



- 
- [11] Neto DM, Martins JMP, Oliveira MC, Menezes LF, Alves JL. Evaluation of strain and stress states in the single point incremental forming process. *Int J Adv Manuf Technol* 2016;85:521-34.
- [12] Bhattacharya A, Maneesh K, Reddy NV, Cao J. Formability and surface finish studies in single point incremental forming. *J Manuf Sci Eng* 2011:133.
- [13] Al-Ghamdi KA, Hussain G. Threshold tool-radius condition maximizing the formability in SPIF considering a variety of materials: experimental and FE investigations. *Int J Mach Tools Manuf* 2015;88:82-94.
- [14] Azevedo NG, Farias JS, Bastos RP, Teixeira P, Davim JP, Sousa RJA. Lubrication aspects during single point incremental forming for steel and aluminum materials. *Int J Precis Eng Manuf* 2015;16:589-95.
- [15] Al-Obaidi A, Kräusel V, Landgrebe D. Hot single-point incremental forming assisted by induction heating. *Int J Adv Manuf Technol* 2016;82:1163-71.
- [16] Khazaali H, Fereshteh-Saniee F. A comprehensive experimental investigation on the influences of the process variables on warm incremental forming of Ti-6Al-4V titanium alloy using a simple technique. *Int J Adv Manuf Technol* 2016;87:2911-23.
- [17] Magnus CS. Joule heating of the forming zone in incremental sheet metal forming: Part 2. *Int J Adv Manuf Technol* 2017;89:295-309.
- [18] Baruah A, Pandivelan C, Jeevanantham AK. Optimization of AA5052 in incremental sheet forming using grey relational analysis. *Measurement* 2017;106:95-100.
- [19] Ambrogio G, Filice L, Gagliardi F. Improving industrial suitability of incremental sheet forming process. *Int J Adv Manuf Technol* 2012;58:941-7.
- [20] Xu D, Wu W, Malhotra R, Chen J, Lu B, Cao J. Mechanism investigation for the influence of tool rotation and laser surface texturing (LST) on formability in single point incremental forming. *Int J Mach Tools Manuf* 2013;73:37-46.